

David W. Hamilton and Fred H. Proctor
NASA Langley Research Center, Hampton, Virginia

1. INTRODUCTION

Aircraft encounters with turbulence are the leading cause of in-flight injuries (Tyrvanas 2003) and have occasionally resulted in passenger and crew fatalities. Most of these injuries are caused by sudden and unexpected encounters with severe turbulence in and around convective activity (Kaplan *et al* 2005). To alleviate this problem, the Turbulence Prediction and Warning Systems (TPAWS) element of NASA's Aviation Safety program has investigated technologies to detect and warn of hazardous in-flight turbulence. This effort has required the numerical modeling of atmospheric convection: 1) for characterizing convectively induced turbulence (CIT) environments, 2) for defining turbulence hazard metrics, and 3) as a means of providing realistic three-dimensional data sets that can be used to test and evaluate turbulence detection sensors. The data sets are being made available to industry and the FAA for certification of future airborne turbulence-detection systems (ATDS) with warning capability.

Early in the TPAWS project, a radar-based ATDS was installed and flight tested on NASA's research aircraft, a B-757. This ATDS utilized new algorithms and hazard metrics that were developed for use with existing airborne predictive windshear radars, thus avoiding the installation of new hardware. This system was designed to detect and warn of hazardous CIT even in regions with weak radar reflectivity (i.e. 5-15 dBz). Results from an initial flight test of the ATDS were discussed in Hamilton and Proctor (2002a; 2002b). In companion papers (Proctor *et al* 2002a; 2002b), a numerical simulation of the most significant encounter from that flight test was presented. Since the presentation of these papers a second flight test has been conducted providing additional cases for examination.

In this paper, we will present results from NASA's flight test and a numerical model simulation of a turbulence environment encountered on 30 April 2002. Progress leading towards FAA certification of industry built ATDS will also be discussed.

2. HAZARD METRIC BACKGROUND

Response of aircraft flying through atmospheric turbulence is dependent upon the fluid scale of motion, aircraft type, altitude, air speed and weight. Therefore, a hazard metric was established to characterize the impact of atmospheric turbulence upon specific aircraft covering its entire flight envelope.

The preferred aircraft turbulence hazard metric is a five second root mean square of the aircraft's normal load; hereafter referred to as RMSg. This metric is preferred because 1) it is airplane centric, 2) easy to

Correlation of Peak Load With Peak RMS Load (5 sec. window)

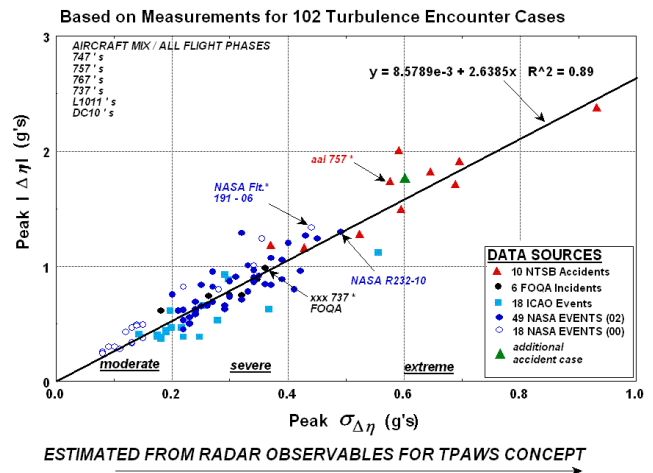


Figure 1. Comparison of the peak load (Δn) to the computed 5-second variance of the peak load ($\sigma_{\Delta n}$) for 102 turbulence encounter cases (provided by Roland Bowles under NASA contract).

calculate, 3) statistically quantifies the sharp bumps and accelerations that passengers feel when flying in an aircraft, and 4) is understood by the airplane operators (Proctor and Hamilton 2005). Within a given turbulence event, the RMSg ($\sigma_{\Delta n}$) is strongly correlated with the peak normal load (Δn) (Figure 1). Because of the known relationship with peak normal load, RMSg hazard levels can be assigned as follows; $0.20 g \leq \sigma_{\Delta n} < 0.30 g$ is moderate and $\sigma_{\Delta n} \geq 0.30 g$ is severe.

The relationship between RMSg and the spectrum width computed by Doppler radar has been shown in Doviak and Lee (1985) and Lee (1977). Therefore, a scientific basis is established for predicting the turbulence impact using a predictive windshear radar.

3. FLIGHT TESTS

NASA installed a candidate ATDS on its own experimental aircraft, a B-757, and flight tested the system on a total of twelve flights; two in the fall of 2000 (Hamilton and Proctor 2002a; 2002b; Proctor *et al* 2002a; 2002b) and the remaining in the spring of 2002 (Hamilton and Proctor 2003). Turbulence events were purposefully encountered by directing the aircraft into convection. During these flights, there were 53 encounters with moderate or greater turbulence. These events usually lasted from a range of several seconds to several minutes and were surrounded by relatively smooth air. Thus, the impact of the turbulence was sudden upon penetration of the convection.

Flight - Event	Altitude (kft)	Weight (klbs)	TAS	Peak In Situ Turbulence (g's)			Peak Vertical Wind (ms^{-1})		Reflectivity (dBz)
				$\sigma_{\Delta n}$	Δn_{max}	Δn_{min}	Max	Min	
190-04	24	184.5	215	0.28	0.58	-0.8	12.15	-6.50	16
190-06	24	183.2	217	0.35	0.71	-1.24	11.18	-6.23	16
191-03	33	179.8	234	0.34	1.00	-0.90	9.32	-15.04	20
191-06	33	177.8	236	0.44	0.87	-1.4	18.41	-14.91	28
227-10	23	171.3	210	0.22	0.37	-0.53	6.74	-2.57	18
228-04	27	182.3	225	0.41	0.63	-0.8	23.42	-4.41	10
228-06	25	181.1	215	0.26	0.66	-0.53	8.79	-10.28	30
228-09	25	179.6	216	0.21	0.47	-0.61	8.45	-4.69	19
228-10	25	178.6	215	0.33	0.56	-0.78	15.69	-5.28	32
228-11	25	177.7	215	0.32	0.65	-0.71	18.70	-2.20	30
228-12	25	176.7	214	0.4	0.7	-1.20	23.25	-4.59	30
229-05	25	179.4	219	0.23	0.51	-0.5	11.25	-7.15	32
230-02	16	192.0	192	0.25	0.4	-0.65	10.62	-6.42	10
230-04	15	188.8	186	0.29	0.63	-0.52	7.60	-10.98	8
230-06	15	187.8	185	0.35	0.92	-0.65	10.80	-12.97	0
230-08	15	187.6	187	0.24	0.63	-0.61	6.84	-12.98	8
230-10	17	186.8	193	0.27	0.95	-0.64	7.49	-9.44	32
230-12	17	186.4	193	0.30	0.73	-0.67	8.52	-11.72	21
230-15	24	183.4	213	0.34	0.86	-0.74	11.02	-7.09	20
230-19	24	181.5	213	0.37	1.02	-1.07	11.17	-12.03	28
230-20	24	180.9	214	0.33	0.71	-1.01	20.71	-4.62	32
230-21	24	180.4	212	0.35	0.65	-0.92	16.25	-6.07	22
230-23	24	179.3	211	0.42	0.79	-0.96	20.37	-14.94	40
230-24	24	178.8	212	0.24	0.47	-0.69	13.64	-4.73	16
231-04	27	186.5	225	0.24	0.61	-0.43	5.84	-5.75	24
231-08	27	184.9	224	0.24	0.58	-0.59	17.10	-3.51	32
231-10	27	184.1	224	0.25	0.61	-0.84	15.21	-3.39	22
231-12	31	180.7	237	0.24	0.58	-0.50	9.40	-5.84	16
232-03	31	182.9	238	0.3	0.69	-0.87	16.27	-8.14	20
232-04	31	182.1	238	0.31	0.91	-0.63	8.53	-8.71	6
232-05	31-35	181.2	227	0.26	0.67	-0.58	7.77	-8.31	4
232-06	35	179.5	236	0.27	0.62	-0.69	5.99	-12.72	2
232-08	35	178.6	235	0.27	0.82	-0.53	7.86	-8.83	8
232-10	35	177.3	235	0.45	1.24	-1.17	14.63	-21.42	22
233-01	28	188.3	227	0.32	1.29	-0.61	15.88	-7.60	22
233-04	17	176.9	194	0.23	0.48	-0.56	5.11	-5.67	4
233-05	17	176.5	194	0.23	0.56	-0.53	6.00	-3.13	10
233-06	17	175.9	195	0.25	0.57	-0.65	4.79	-7.73	18
233-07	17	174.9	193	0.39	0.89	-0.65	11.73	-7.10	22
233-09	17	172.7	194	0.24	0.58	-0.55	10.43	-5.92	16
234-05	25	180.0	219	0.20	0.76	-0.34	5.80	-3.16	13
234-06	25	179.0	218	0.43	1.27	-1.12	14.43	-9.36	22
234-09	25	175.4	219	0.29	0.65	-0.65	9.34	-7.17	16
234-11	25	174.1	220	0.34	0.97	-0.89	12.38	-8.86	24
234-12	25	173.5	218	0.34	0.86	-0.90	12.54	-7.71	22
235-02	26	179.6	224	0.23	0.43	-0.50	8.45	-4.33	22
235-03	24	178.7	216	0.36	0.81	-0.85	17.76	-7.39	32
235-05	22-19	170.9	204	0.22	0.45	-0.39	11.07	-4.88	2
235-07	19	169.4	201	0.22	0.46	-0.62	8.27	-3.04	24
235-08	19	168.4	201	0.37	0.84	-1.14	14.18	-6.08	8
235-09	19	167.7	200	0.23	0.51	-0.41	2.77	-10.99	8
240-03	29	181.7	235	0.39	0.96	-1.06	14.98	-2.35	4
240-09	25	179.4	218	0.49	1.30	-1.07	22.13	-2.09	32

Table 1. Summary of NASA's 53 significant turbulence events

Details of the turbulence encounters are listed in Table 1. In situ measurements from NASA's B-757 also were analyzed to assist in the characterization of turbulence and to aid in the evaluation of the ATDS. Examination of the performance of the ATDS during the second campaign was very encouraging. Of the 49 encounters with moderate to severe turbulence, 81% of the events were predicted 30 seconds or more prior to encounter (Bowles *et al* 2002). These successful warnings often occurred with weak radar reflectivity. Several of the turbulence events had radar reflectivity levels that provided no reflectivity target on the crew's cockpit display.

3.1 Radar Reflectivity

A general aviator's rule of thumb in preventing turbulence accidents is to avoid convective activity. Operationally, this is not always achievable due to large masses of atmospheric convection, for which avoidance can greatly affect airliner capability to meet schedules and to reduce fuel consumption. Also, it is believed that avoiding areas of high radar reflectivity (> 40 dBz) may avert most of the hazardous turbulence. However, as will be shown, our flight tests indicate that hazardous turbulence can be found at any radar reflectivity.

From the flight test data, Figure 2 reveals a weak, but poor correlation between radar reflectivity and the RMSg. Note that some of the more intense events were not in environments with high levels of radar reflectivity, and many of the events occurred within radar reflectivity below the threshold of the aircraft radar display; i.e. <20 dBz.

3.2 Radar Prediction of Normal Loads

Doppler radar systems detect components of motion along the direction of the radar beam, while aircraft primarily respond to fluctuations in the vertical wind. Therefore, assumptions must be made in order to convert radar measurements into an aircraft hazard metric. If atmospheric turbulence were truly isotropic at the scale of the radar pulse volume, then one would expect perfect correlation between the statistics of these two wind components. However, the isotropy assumption may be violated as deduced from the in situ data collected by NASA's B-757.

The anisotropic tendency of the convective turbulence environments is apparent in Figure 3. The variances were calculated for in situ measurements of vertical wind (w) and head wind (u), components. In most of the events, values of σ_w are greater than σ_u , which is consistent with other research on turbulence within convective clouds (Steiner and Rhyne 1962).

Another issue for hazard detection with radar is the displacement between peak σ_u (which is more or less oriented along the direction of the radar beam) and σ_w (the vertical component which affects the response of the aircraft). The reason that the two parameters are not collocated can be attributed to the turbulence length-scale as well as anisotropy of the turbulence. In roughly half the cases, the displacement (L_x) between peak σ_u and σ_w is greater than 400m (Figure 4). However, in

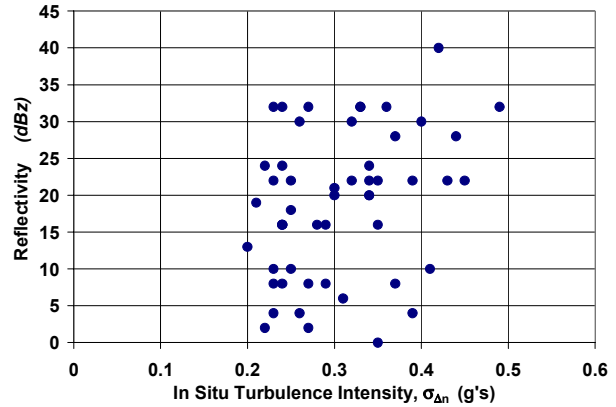


Figure 2. Peak radar reflectivity along flight path for the events listed in Table 1.

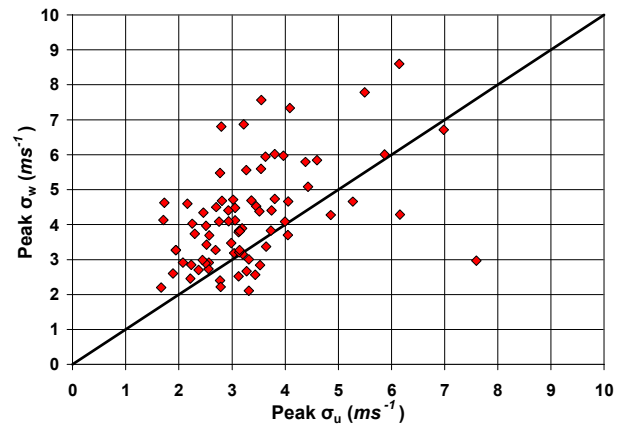


Figure 3. Corresponding peak values of headwind variance (σ_u) and vertical wind variance (σ_w) measured in situ for all 2002 turbulence events (Flights 227 – 240). Variances were computed using a 5 second window.

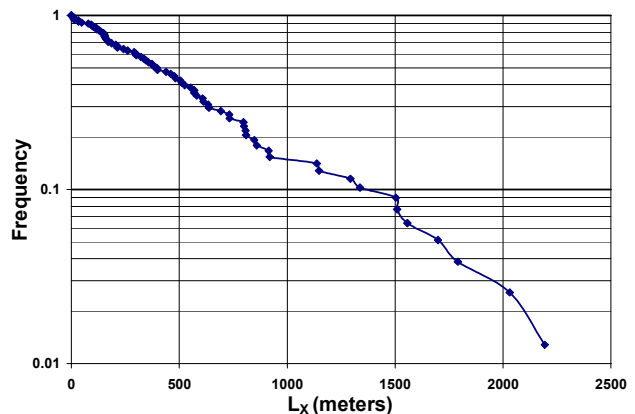


Figure 4. Frequency distribution of the distance between peak values of σ_u and σ_w for events presented in Figure 3.

nearly all of the events the displacement was less than 2 km. Therefore, an alerting strategy must consider this displacement between the sensed and actual hazard.

4.0 TURBULENCE EVENT 232-10

Event 232-10 began at 1913 UTC on April 30, 2002 while NASA's B-757 was encountering a convective complex located over north-central Alabama. Composite radar reflectivity from the Huntsville, AL NEXRAD (Polger 1994) shows the line of convective cells across Alabama (Figure 5). Storm tops were between 10 and 12 km (35,000 and 40,000 ft) and cell motion was towards the east-southeast at 40 ms^{-1} . Ambient winds at flight level, $\sim 10.5 \text{ km AGL}$, were from the west-northwest at 50 ms^{-1} (100 kts), with significant vertical shear near the upper portions of the storm. An airmet for moderate turbulence had been issued indicating wide-spread turbulence in association with the vertical wind shear at the jet stream levels.

Extensive outflow from large cells located upstream of the complex led to instrument meteorological conditions (IMC) for most of the data collection period (Figure 6).

The severe turbulence encounter was associated with the penetration of a rapidly rising convective plume within the complex. Very weak radar reflectivity was associated with the plume with no evidence of a return on the ship's radar display.

Event 232-10 exemplifies the operational environment in which accidents occur due to turbulence. The flight environment was IMC, so 'see and avoid' was not an option, the convection was not displayed on ship's radar ($< 20 \text{ dBz}$), the encounter was sudden, of short duration, and of severe intensity. Also, no reports of severe turbulence were made prior to the time of the event. However, soon after the NASA aircraft experienced the event, two commercial aircraft, an MD-80 and an A319, both reported severe turbulence within 10 km and 30 min of event 232-10.

Associated radar reflectivity factor and RMSg fields are presented in Figure 7 and Figure 8, respectively. Radar reflectivity associated with the convective plume is generally less than 20 dBz. The turbulence intensities predicted by the ATDS (Figure 8) indicated a continuous 20 km path of moderate and often severe turbulence ahead of the aircraft. The predicted intensities are validated with measurements in situ presented in Figure 9.

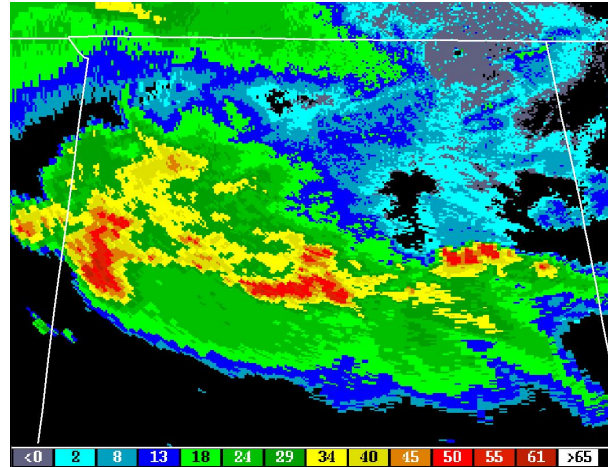


Figure 5. NEXRAD composite radar reflectivity (dBz) from the Huntsville, AL radar at 19:12:34 UTC on 30 April 2002. The high reflectivity cell located in the middle of the figure was penetrated by NASA's B-757 and is the subject of this study.

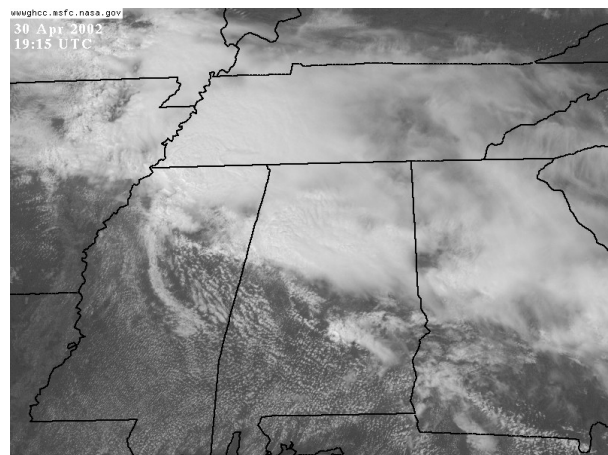


Figure 6. GOES-12 Visible satellite image at 1915 UTC on 30 April 2002.

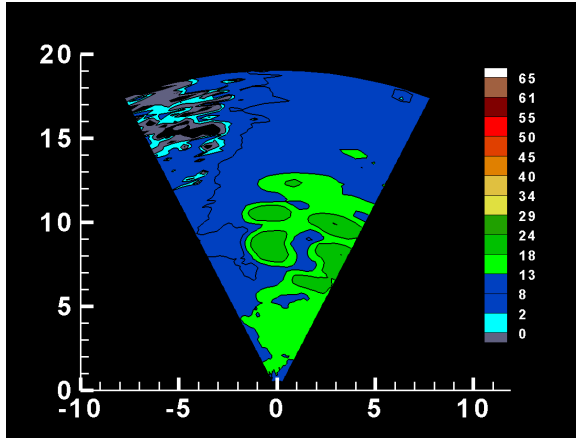


Figure 7. Airborne radar reflectivity factor (dBz) observed by NASA's B-757 for Event 232-10. Coordinates are in units of km.

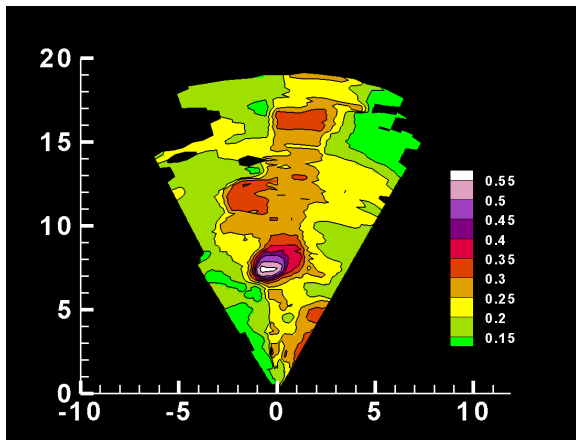


Figure 8. Same as in Figure 7 but for ATDS predicted RMSg.

4.1 Numerical Simulation of Event 232-10

Numerical modeling of the convective complex associated with this turbulence event is conducted using NASA's Terminal Area Simulation System (TASS) (Proctor 1987; 1996). TASS is a large eddy simulation (LES) model developed for simulating convective clouds, atmospheric turbulence, and aircraft wake vortex behavior. Validation of the numerical simulations has included measurements in situ, as well as measurements from ground-based NEXRAD radar and from airborne radar. Previously, this model was applied to another NASA turbulence encounter as detailed in Proctor *et al* (2002a; 2002b). Further details of the model formulation can be found in references (Proctor 1986; DeCroix 2001).

4.1.1 Model Domain, Boundary, and Initial Conditions

Numerical simulation of the event requires appropriate initial conditions, and specification of a physical domain with sufficient grid resolution to resolve

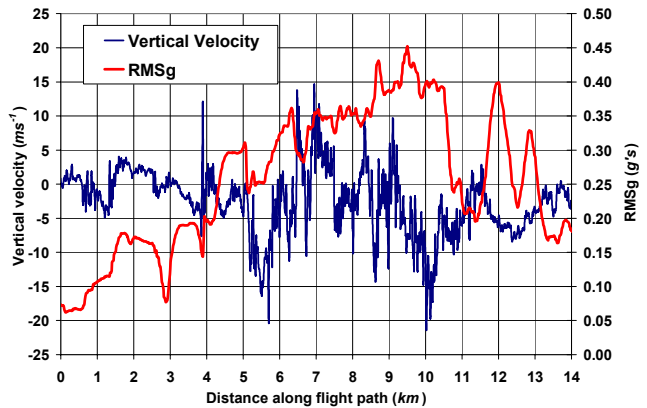


Figure 9. Measurements in situ of vertical wind and RMSg along the flight path for Event 232-10.

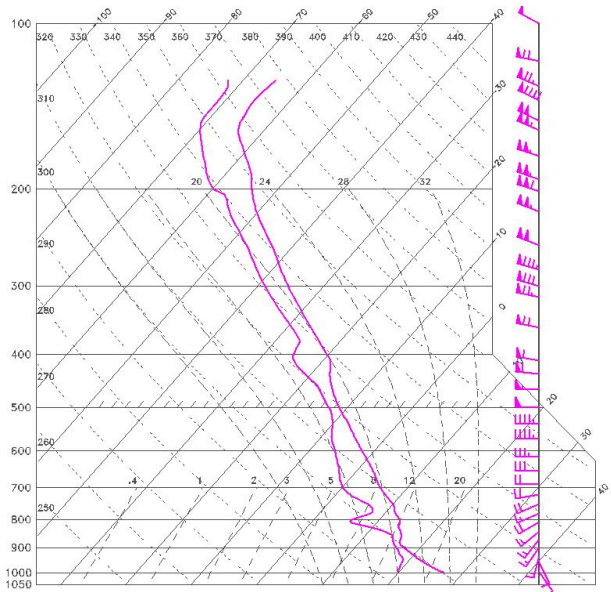


Figure 10. Skew-T for time and location near Event 232-10.

the important scales of turbulence. The assumed domain size is 20 km x 30 km x 14.75 km, with periodic conditions assumed on the eastern and western edges of the grid. The number of grid points in the domain is 254 x 378 x 178, with a horizontal grid spacing of 80 m. The vertical grid size stretches with height. The domain is rotated 12 degrees clockwise to account for mean storm motion. The initial environmental conditions (Figure 10) were extracted from the Mesoscale Analysis and Prediction System (MAPS) forecast near time and location of event. MAPS is the experimental version of the Rapid Update Cycle (Benjamin 2002). Obtaining initial conditions that represent the environment of the storm is critical to the success of the numerical simulation.

Variable	TASS		Observed	
Peak Storm Tops	11 km		10-12 km	
Peak Radar Reflectivity near Flight Level	17.5 dBZ		18 dBZ from aircraft	
Cell Motion (toward)	ESE at 35 ms^{-1}		ESE at 40 ms^{-1}	
Width of Convective Line near Ground (based on 20 dBZ)	11 km		15-25 km	
Peak Vertical Velocity near Flight Level	Max 11 ms^{-1}	Min -11 ms^{-1}	Max 15 ms^{-1}	Min -21 ms^{-1}
Horizontal Scale of Turbulence Patch near Flight Level	3-5 km		8 km	

Table 2. Comparison of simulated and observed characteristics for Event 232-10.

4.1.2 Results of the Numerical Simulation

Comparisons of key parameters between observed and simulation for Event 232-10 are presented in Table 2.

A simulated radar reflectivity field compares well with the observed NEXRAD imagery from Huntsville, AL, which is shown in Figure 11.

The TASS simulation indicates overshooting tops with strong horizontal gradients of vertical velocity. Associated with these overshooting tops are regions of weak radar reflectivity, as they are composed of small ice and snow hydrometeors.

4.1.3 Hazard Analysis

The hazard field diagnosed from the numerical simulation of Event 232-10 is shown in Figure 12. The RMSg was estimated using the Moving Box Method described in Proctor *et al* (2002a; 2002b). A peak σ_w value of 8.2 ms^{-1} is calculated from the numerical simulation at the flight level of 10.5 km. Applying NASA's B-757 hazard algorithm (Bowles 2003) for the corresponding weight, altitude, and airspeed from Event 232-10, the RMSg is 0.38, i.e. severe turbulence.

4.1.4 Radar Simulation

A radar simulation is conducted in order to demonstrate its value in evaluating hazard algorithms. The radar simulation is conducted using a data set extracted from the numerical simulation of Event 232-10. The radar simulation is performed with the Airborne Doppler Weather Radar Simulation (ADWRS) system, which was initially developed for NASA's Airborne Windshear Program (Switzer and Britt 1996; Arbuckle *et al* 1996). Results of the airborne radar simulation are shown in Figure 13 and Figure 14.

As in the actual event, severe turbulence intensities are predicted in regions of weak radar reflectivity, i.e. less than 20 dBz.

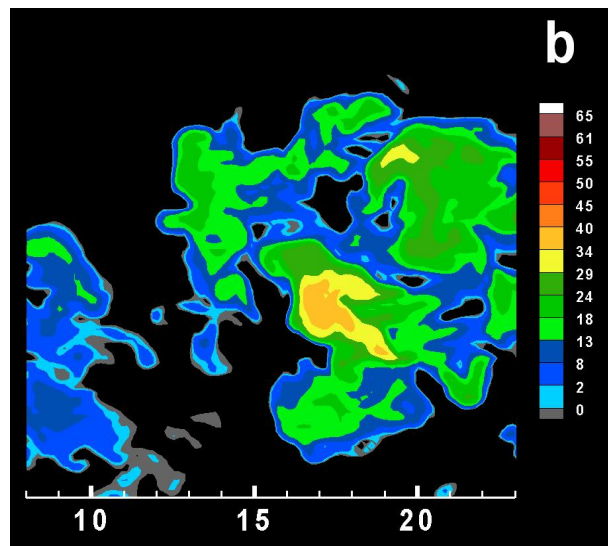
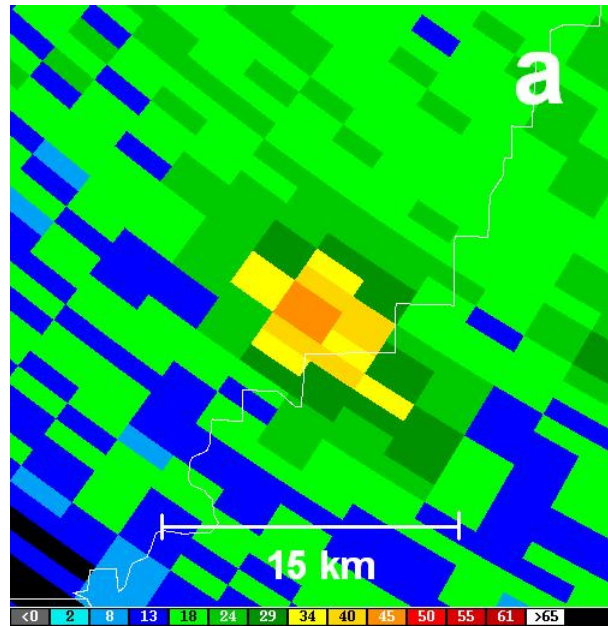


Figure 11. Radar reflectivity factor (dBz) from a) the 2.4 degree scan from the Huntsville, AL NEXRAD radar at 19:13 UTC 30 April 2002 and b) a tilted horizontal plane representing a 2.4 degree scan through the TASS simulation at 51 minutes (Coordinate units are in km).

The radar simulated RMSg in Figure 14 correlates excellently with the hazard diagnostic shown in Figure 12. Although the peak RMSg intensities for the radar predicted and the Moving Box method are not collocated, the positions are no more than about 2 km, which is consistent with flight data (Figure 4). Furthermore, peak magnitudes differ by only 10% (see Table 3).

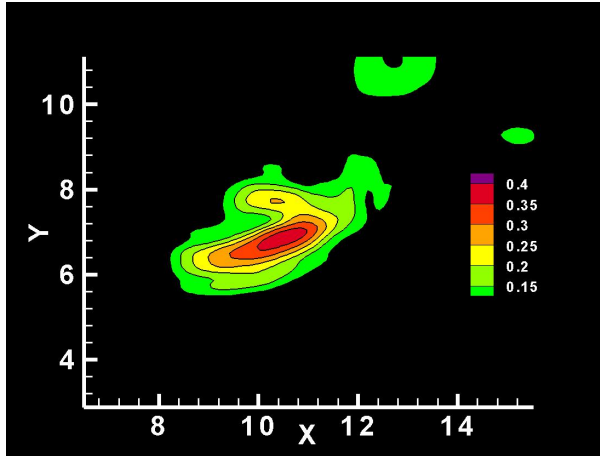


Figure 12. Hazard field diagnosed from numerical simulation of Event 232_10. Units are in RMSg. Field depicted for a horizontal plane at 10.3 km AGL. (Coordinate units are in km).

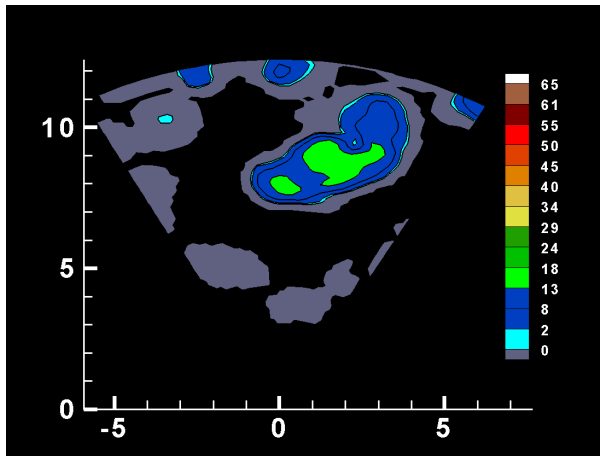


Figure 13. ADWRS Simulated airborne radar reflectivity facto (dBz) using 232-10 numerical data set. Assumes aircraft approaching from south at an altitude of 10.3 km AGL. (Coordinate units are in km)

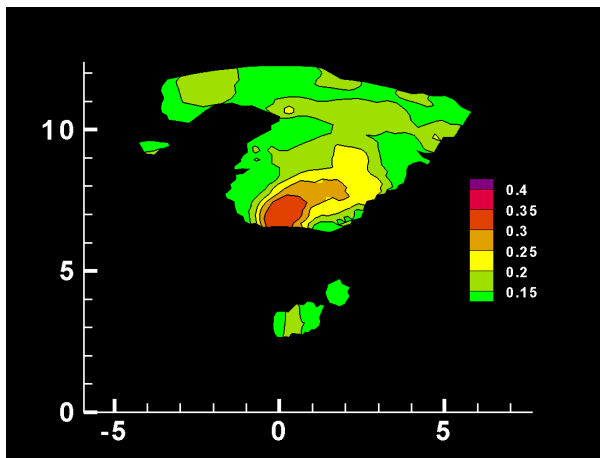


Figure 14. Same as Figure 13 but for ATDS simulated RMSg.

Source	Peak $\sigma_{\Delta n}$ (g's)
In situ	0.44
Onboard Turbulence Radar	0.55
Model Diagnostic from σ_w field	0.38
Radar Simulation with Model Data	0.34

Table 3. RMSg Comparison

4.1.5 RMSg Comparison

Table 3 shows comparisons between the peak RMSg measured by the B-757 in situ and airborne radar with those simulated from the numerical data set. All sources indicate a severe turbulence event, whether from observed data or simulation.

5.0 Certification

Since new ATDS may incorporate alerting functionality, requiring flight crews to take procedural action in the event of a potentially hazardous turbulence encounter, radar manufactures are expected to file for FAA certification. Therefore, this and other data sets have been made available to FAA and industry for algorithm testing and certification support.

A tool set has been made available for the certification effort, which includes numerically-simulated data sets of CIT environments. The Moving Box Method analysis has been accepted for characterizing the 'truth' hazard within the data sets. The tool set also includes hazard tables for a number of commercial transport aircraft, and the ADWRS radar simulation system. All components of the tool set have been delivered to the FAA and are available to industry for development and testing of radar-based ATDS (Hamilton and Proctor 2005).

6.0 Summary and Discussion

Measurements of convectively induced turbulence were gathered during twelve NASA research flights. On these flights, convection was purposefully penetrated to make radar detections of CIT. Measurements in situ were used to evaluate the performance of the ATDS hazard algorithm. The hazard algorithm performance during the 2002 flight campaign was promising. The algorithm predicted the impact of the turbulence upon the aircraft with an 81% probability of detection, even though regions of high reflectivity (>40 dBz) were avoided.

Turbulence intensity was only weakly correlated with radar reflectivity factor, indicating that the level of radar reflectivity is not a good measure of the turbulence threat. In several of the turbulence encounters, the radar reflectivity was lower than the ship's radar display threshold (<20 dBz). Thus avoiding regions of high radar reflectivity does not mitigate the risk of dangerous CIT, and a successful ATDS must be able to perform in low radar reflectivity.

Statistics of the NASA in situ turbulence measurements revealed anisotropic characteristics of the turbulence environments. However, analyses showed that on the aircraft path, peak variances in the

vertical wind component were typically located within 2 km of the peak variance in the head wind component.

A cloud-scale, LES of the convective system responsible for turbulence event 232-10 was conducted and compared with observational data. Results from the simulation compared well with airborne and ground-based radar data. RMSg values were diagnosed with a hazard estimation model and predictions of the hazard were made with an airborne radar simulation of the 232-10 data set. RMSg values from the hazard diagnostic and the radar simulation compare reasonably well with the observed values. All sources indicate a severe turbulence event.

The LES data set, hazard metric model, and the in situ analyses are shown to be useful tools for characterizing CIT and for evaluating turbulence detection sensors. Also, these tools can be useful in certification of future ATDSs.

7.0 References

- Arbuckle, P.D., M. S. Lewis, and D. A. Hinton, 1996: Airborne Systems Technology Application to the Windshear Threat. *20th Congress of the International Council of the Aeronautical Sciences*, Sorrento, Italy, ICAS Paper No. 96-5.7.1, pp. 1640-1650.
- Benjamin, S.G., S.S. Weygandt, B.E. Schwartz, T.L. Smith, T.G. Smirnova, D. Kim, G. Grell, D. Devenyi, K.J. Brundage, J.M. Brown, and G.S. Manikin, 2002. The 20-km RUC in Operations. *Preprints, 15th Conf. on Numerical Weather Prediction*, San Antonio, TX, Amer. Meteor. Soc., pp. 379-382.
- Bowles, R.L., D.W. Hamilton, and L. Cornman, 2002: FY02 TPAWS Radar NASA B757 Flight Campaign Summary. Oral Presentation, NASA's Annual Weather Accident Prevention Review, Lexington, MA. Powerpoint Presentation available at: <http://wxap.grc.nasa.gov/review/2002.html>
- Bowles, R.L., 2003: Hazard Metric Data. Available at: http://tpaws.larc.nasa.gov/flight_data/TPAWS_Certificati_on_Tool_Set/Hazard_Metric_Data/
- DeCroix, D.S., 2001. *Large-Eddy Simulations of The Convective and Evening Transition Planetary Boundary Layers*. Ph.D. Dissertation, North Carolina State University, Raleigh, N.C., 275 pp.
- Doviak, R. J., and J. T. Lee, 1985: Radar for Storm Forecasting and Weather Hazard Warning. *J. Aircraft*, **22**, 1059-1063.
- Hamilton, D.W., and F.H. Proctor, 2002. Convectively Induced Turbulence Encounters During NASA's Fall 2000 Flight Experiments. *Preprints, 10th Conference on Aviation, Range, and Aerospace Meteorology*, Portland, OR, Amer. Meteor. Soc., pp. 371-374.
- Hamilton, D.W., and F.H. Proctor, 2002: Meteorology Associated with Turbulence Encounters During NASA's Fall-2000 Flight Experiments. *40th Aerospace Sciences Meeting and Exhibit*, AIAA-2002-0943, 11pp.
- Hamilton, D.W., and F.H. Proctor, 2003. An Aircraft Encounter with Turbulence in the Vicinity of a Thunderstorm. *21st AIAA Applied Aerodynamics Conference*, AIAA-2003-4075, 11pp.
- Hamilton, D.W., and F.H. Proctor, 2005: Certification Methodology & Tools for Airborne Turbulence Detection Systems. Oral Presentation, NASA Weather Accident Project Review, Williamsburg, VA. Powerpoint Presentation available at: <http://wxap.grc.nasa.gov/review/2005.html>.
- Kaplan, M.L., A.W. Huffman, K.M. Lux, J.J. Charney, A.J. Riordan, and Y.-L. Lin, 2005: Characterizing the severe turbulence environments associated with commercial aviation accidents. *Meteorol. Atmos. Phys.*, **88**, 129-152.
- Lee, J. T., 1977: Application of Doppler Radar to Turbulence Measurements Which Affect Aircraft. Final Rep. No. FAA-RD-77-145. FAA Syst. Res. Dev. Serv., Washington, D.C.
- Polger, P.D., B.S. Goldsmith, R.C. Przywarty, and J.R. Bocchieri, 1994. National Weather Service warning performance based on the WSR-88D," *Bull. Amer. Met. Soc.*, **75**, 203-214.
- Proctor F.H., 1987: The Terminal Area Simulation System, Volume 1: Theoretical Formulation. NASA Contractor Report 4046, DOT/FAA/PM-85/50, 1, 176 pp.
- Proctor, F.H., 1996. Numerical Simulation of Wake Vortices During the Idaho Falls and Memphis Field Programs. *14th AIAA Applied Aerodynamics Conference*, AIAA-96-2496, pp. 943-960.
- Proctor, F.H., D.W. Hamilton, and R.L. Bowles, 2002. Numerical Simulation of a Convective Turbulence Event. *Preprints, 10th Conference on Aviation, Range, and Aerospace Meteorology*, Portland, OR, Amer. Meteor. Soc., May 2002, pp. 41-44.
- Proctor, F.H., D.W. Hamilton, and R.L. Bowles, 2002. Numerical Study of a Convective Turbulence Encounter. *40th Aerospace Sciences Meeting and Exhibit*, AIAA-2002-0944, 14pp.
- Proctor, F.H. and D.W. Hamilton, 2005: Turbulence Hazard Metric Unification. Oral Presentation, NASA Weather Accident Project Review, Williamsburg, VA. Powerpoint Presentation available at: <http://wxap.grc.nasa.gov/review/2005.html>.
- Steiner, R. and R.H. Rhyne, 1962. Some Measured Characteristics of Severe Storm Turbulence," Nat. Severe Storm Project, Rep. No. 10, p. 17.

Switzer G. F. and C. L. Britt, 1996: Performance of the NASA Airborne Radar With the Windshear Database for Forward-Looking Systems , NASA CR-201607, pp. 85.

Tvaryanas AP, 2003. Epidemiology of Turbulence-Related Injuries in Airline Cabin Crew, 1992–2001. *Aviat Space Environ Med*, **74**, 970–976.